Polarization state of the output of soft-x-ray lasers through the paraxial Maxwell-Bloch approach

D. Benredjem, A. Sureau, B. Rus,* and C. Möller
Laboratoire de Spectroscopie Atomique et Ionique, URA 775 du CNRS, Université Paris–Sud, Bâtiment 350, 91405 Orsay Cedex, France
(Received 2 June 1997)

The polarization state of the output of collisionally pumped soft-x-ray lasers is studied through the Maxwell-Bloch (MB) approach considering level degeneracy. We have used the MB theory, so as to account for the propagation of linearly polarized waves, in the laser-target conditions of two recent experiments on neonlike germanium. In the case where a linearly polarized x-ray beam is injected into an amplifying plasma, we conclude that the polarization state of the output will be basically unaltered by the amplifier. We have also investigated intrinsic polarization of the output of an amplified-spontaneous-emission system, i.e., in the absence of a seeded radiation. Applied to the $J=0-J=1$ lasing line, the calculations suggest that the emerging signal is not polarized. However, one of the experiments referred to above has shown a spontaneous polarization, but the mechanism invoked by the authors to interpret this result, namely a selective trapping of the resonance line, is shown to be negligible, especially when elastic electron-ion collisions are taken into account. The influence of these collisions on the polarization properties of the amplifier is investigated through the atomic orientation and alignment. A spontaneous contribution to the output polarization is obtained when a circularly polarized beam is injected in the amplifier in order to create the necessary population differences between the quantum states of each laser level. [S1050-2947(97)07512-4]

PACS number(s): 42.55.Vc, 42.25.Ja, 32.80.−t

I. INTRODUCTION

Soft-x-ray amplification in collisionally pumped lasers has been demonstrated in Ne-like Se in 1985 [1], and since then continuing effort has been devoted to the development of (i) systems producing a strongly amplified radiation, and (ii) high-performance lasers, i.e., control and optimization of x-ray beams. In these attempts, the collisional excitation is today the most efficient and robust scheme. Strong amplification at wavelengths ranging from 84.7 nm in Si [2] to 3.5 nm in Au [3] has been demonstrated, while, in a capillary-discharge system, gain-length products greater than 25 have been obtained at 46.9 nm in Ar by Rocca and co-workers using double pass amplification [4]. Saturation has been reported in neonlike Zn [5], Ge [6], Se [3], Y [7], and in nickel-like Ag [8,9].

With adequate irradiance conditions inversions may be obtained for various $(2p_{j1}^5 3p_{j2})_J-(2p_{j1}^5 3s_{1/2})_{J'}$ transitions in Ne-like ions, the strongest of which are generally with $J=0$, $J'=1$ (henceforth called 0-1) and with $J=2$, $J'=1$ (hereafter called 2-1). The $J=0$ levels cannot decay by radiative transition to the $(2p^6)_0$ ground state, while the $J=2$ levels can, but only via electric-quadrupole transition. The levels involved in lasing are strongly populated by electron collisions (mainly from the ground state), and inversions can occur, due to the fast radiative decay of the lower levels. The purpose of this work is to study the possible development of a polarization of the x-ray beam in the framework of the paraxial Maxwell-Bloch (MB) theory, which is well suited for the study of strongly inverted media. The level degeneracy must be explicitly considered to take into account the specific interaction of the amplified radiation with each of the involved quantum states.

Polarization and spatial coherence may be important in many applications involving extreme ultraviolet (XUV) radiation. Generally x-ray lasers operating in the amplified-spontaneous-emission (ASE) regime provide unpolarized beams. However, Kieffer *et al.* [10] have observed a polarized emission from an Al plasma produced by a 1-ps laser pulse. The authors have explained their result as due to spatial anisotropy in the velocity distribution of the plasma electrons. The theoretical model developed in this work is applied to experiments involving polarized x-ray lasers produced from collisionally excited neonlike Ge.

Rus *et al.* [11] studied the polarization of two 2-1 ASE output lines of wavelengths of 23.2 and 23.6 nm, and the amplification of a linearly polarized 2-1 beam at 23.6 nm in an injector-amplifier configuration. The ASE polarization properties were examined using a double plasma of 44-mm composite length, produced by irradiating 100-μm-wide Ge stripes by laser pulses delivering $\sim 1.6\times 10^{13}$ W cm^{-2} over ~ 650 ps [full width at half maximum (FWHM)] at a wavelength of 1.06 μm. The attained gain-length product was ~ 15.5, implying an ASE system close to the saturation threshold. From the data assembled it was concluded that, under the conditions of the experiment, there is no preferred, systematic direction of polarization in the ASE output, and that, within the accuracy of the measurement (5%), the time-integrated degree of polarization of the beam is zero. In order to study the amplification of polarized radiation, the ASE output was linearly polarized to a degree of polarization of 0.97 and injected into an additional 14-mm-long Ge plasma driven at $\sim 1.3\times 10^{13}$ W cm^{-2}. Taking into account the throughput and polarization properties of the optics, the beam was seeded with a gain length of 8. The degree of polarization of the amplifier output, emerging with a gain-

*Permanent address: Gas Lasers Department, Institute of Physics, 18040 Prague 8, Czech Republic.

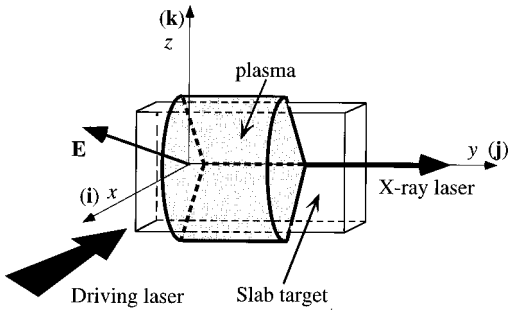

FIG. 1. Schematic representation of the interaction of a pump laser with a slab target. The nearly cylindrical produced plasma expands in the direction of the pump laser. The y axis is taken to be the propagation axis of the x-ray beam, and the electric field is thus contained in the transverse plane xz. **i**, **j**, and **k** are the unit vectors of a right-handed orthonormal basis.

length product of ~ 12, has been measured to be $0.98^{+0.02}_{-0.05}$, i.e., identical, within the experimental precision, to the degree of polarization of the injected beam.

In the work of Kawachi *et al.* [12], the polarization state of the 19.6-nm 0–1 ASE output of a 3-cm-long Ge plasma has been examined. The plasma was created by two 100-ps Gaussian pulses 400 ps apart. The irradiance produced by the second pulse, during which strong amplification at 19.6 nm occurred, was, according to the shot configuration, 2.9×10^{13} or 3.2×10^{13} W cm^{-2}. The ASE output was seen to be polarized in the direction perpendicular to the target surface, with its degree of polarization strongly depending on the irradiance. The polarization was attributed in Ref. [12] to the anisotropy of the gain coefficient, radiation trapping of the resonance line $(2p^6)_0-(2p^5_{1/2}3s_{1/2})_1$ being different in the directions parallel and perpendicular to the target. This is assumed to occur as a consequence of a higher Doppler decoupling in the perpendicular direction, resulting from a velocity gradient higher in this direction than in the direction parallel to the target. Thus the $(2p^5 3s)$ ions with quantum numbers $J=1$ and $M=\pm1$ would experience less radiation trapping than those with quantum numbers $J=1$ and $M=0$.

The diagram of the pump laser-slab target interaction that gives rise to an elongated plasma is shown in Fig. 1. The obtained plasma is assimilated into a cylindrical column whose axis is taken to be the y axis. Spontaneous emission between an upper level u and a lower level l could be amplified through the process of stimulated emission if a population inversion occurs between u and l. The time-dependent monochromatic intensity $I(\nu,y,t)$ of a radiation propagating along increasing y is the solution of the radiative-transfer equation. In many situations involving radiation transport, and relevant to x-ray laser modeling as well as to astrophysics, the problem is to find the solution of the one-dimensional (1D) equation

$$\frac{\partial}{\partial y} I(\nu,y,t)=G(\nu,y,t)[I(\nu,y,t)+S(\nu,y,t)], \qquad (1)$$

where G and S designate the local gain (cm^{-1}) and the source function, respectively. In x-ray lasers G involves absorption and induced emission. The above equation is coupled to the rate equations governing the evolution of the population densities N_i,

$$\frac{\partial}{\partial t} N_i(y,t)=-N_i(y,t)\Gamma_i(y,t)+r_i(y,t), \qquad (2)$$

where i designates quantum states of the lasing ions. Γ and r are, respectively, the total decay rate of the i state and the sum of all processes populating it. The need to take level degeneracy into account leads us to consider the quantum-state populations instead of the level populations. Calculations follow the method developed in a recent work on the transition from ASE to the saturation regime [13], and are presented in the next section.

II. COLLISIONAL-RADIATIVE EQUATIONS

The propagation of a radiation through a globally neutral plasma obeys the Maxwell wave equation

$$\Delta\mathbf{E}-\frac{1}{c^2}\frac{\partial^2}{\partial t^2}\mathbf{E}-\frac{\omega_{pe}^2}{c^2}\mathbf{E}=\frac{1}{\varepsilon_0 c^2}\frac{\partial^2}{\partial t^2}\mathbf{P}, \qquad (3)$$

where $\mathbf{E}=\mathbf{E}(x,y,z,t)$ is the electric field, $\mathbf{P}=\mathbf{P}(x,y,z,t)$ the polarization vector, and $\omega_{pe}=[N_{\rm elec}q^2/(\varepsilon_0 m_e)]^{1/2}$ the electron plasma frequency ($N_{\rm elec}$ being the free-electron number density).

The electric field of waves propagating along the y axis (see Fig. 1) is such that $E_y=0$. In the absence of incident radiation, the x and z components have the same amplitude because x- and z-polarized radiations have equal spontaneous-emission probabilities. As transverse fields are real we can write

$$E_x=E\ \sin(\omega t-ky), \quad E_z=E\ \sin(\omega t-ky+\varphi).$$

The x component can be expressed as a coherent superposition of a τ_+ and a τ_- electric field, and the z component is represented by a π wave. So, equivalently, we can consider

$$\mathbf{E}_{\sigma+}=\frac{E}{2}\cos\left(\omega t-ky-\frac{\pi}{2}\right)\mathbf{i}+\frac{E}{2}\sin\left(\omega t-ky-\frac{\pi}{2}\right)\mathbf{j}, \qquad (4a)$$

$$\mathbf{E}_{\sigma-}=-\frac{E}{2}\cos\left(\omega t-ky+\frac{\pi}{2}\right)\mathbf{i}+\frac{E}{2}\sin\left(\omega t-ky+\frac{\pi}{2}\right)\mathbf{j}, \qquad (4b)$$

$$\mathbf{E}_{\pi}=E\ \sin(\omega t-ky+\varphi)\mathbf{k}, \qquad (4c)$$

where $k=\omega/c$ is the wave vector and **i**, **j**, **k** the unit vectors of a right-handed orthonormal basis. A relation between the above elementary fields and the $\Delta M[=M_u-M_l]$ values, the M's being the magnetic quantum numbers, can be easily established if these fields are expressed in a tensorial form, i.e.,

$$\mathbf{E}_{\sigma+}=\frac{E}{2\sqrt{2}}[-e^{i(\omega t-ky-\pi/2)}\mathbf{e}_1+e^{-i(\omega t-ky-\pi/2)}\mathbf{e}_{-1}], \qquad (5a)$$

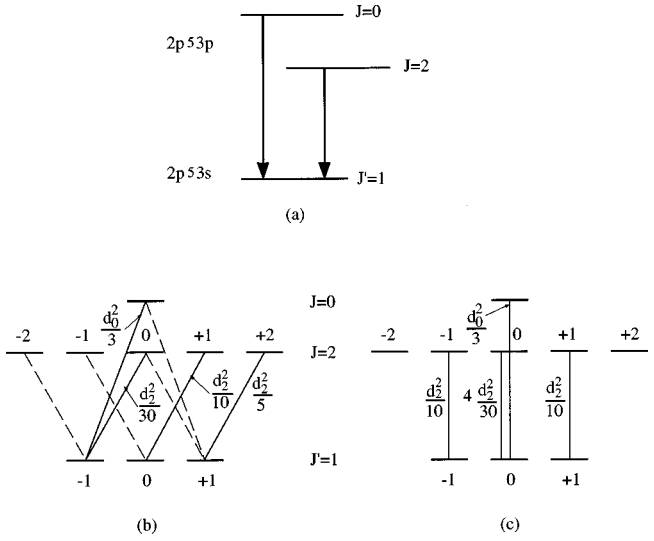

FIG. 2. Diagram of the energy levels (a) and quantum states (b), (c) involved in the 0-1 and 2-1 radiations. In (b) we show the transitions giving rise to right (solid lines) and left (dashed lines) circularly polarized radiation. Transitions giving rise to linear polarization are shown in (c). We give for τ_+ waves the values of $\langle JM|d_1|J'M-1\rangle^2$ in terms of the reduced matrix element $d_J=(J\|d\|J'=1)$. The appropriate values for the τ_- waves are $\langle JM|d_{-1}|J'M+1\rangle^2$. They are obtained from the relation $\langle JM|d_{-1}|J'M+1\rangle^2=\langle J-M|d_1|J'-M-1\rangle^2$. In (c) we give the $\langle JM|d_0|J'M\rangle^2$ values that correspond to the $\Delta M=0$ transitions.

$$\mathbf{E}_{\sigma-}=\frac{E}{2\sqrt{2}}\,[e^{-i(\omega t-ky+\pi/2)}\mathbf{e}_1-e^{i(\omega t-ky+\pi/2)}\mathbf{e}_{-1}], \quad (5b)$$

$$\mathbf{E}_{\pi}=\frac{E}{2i}\,[e^{i(\omega t-ky+\varphi)}-e^{-i(\omega t-ky+\varphi)}]\mathbf{e}_0, \quad (5c)$$

where $\mathbf{e}_{\pm1}[=(\mp\mathbf{i}+i\mathbf{j})/\sqrt{2}]$ and $\mathbf{e}_0(=\mathbf{k})$ are the new unit vectors. $\mathbf{e}_{\pm1}$ is associated with $\Delta M=\pm1$ transitions, while $\mathbf{e}_0$ involves $\Delta M=0$ transitions (see Fig. 2). As a result, the MB calculations are greatly simplified.

The polarization vector is given by $\mathbf{P}=\mathrm{Tr}(\rho\mathbf{d})$, where ρ is the density-matrix operator and $\mathbf{d}$ the electric dipole of the emitter. At $t=0$ the coherences (nondiagonal elements of ρ) are equal to zero and ρ may hence be written

$$\rho=\sum_{JM}\,|JM\rangle\langle JM|n_{JM}, \quad (6)$$

where $n_{JM}[=\rho_{JM,JM}=\langle JM|\rho|JM\rangle]$ is the fractional-population density of the $|JM\rangle$ state. We then consider the Bloch relation

$$i\hbar\,\frac{\partial}{\partial t}\,\rho=[H,\rho], \quad (7)$$

where $H=H_A-\mathbf{d}\cdot\mathbf{E}$, with H_A designating the Hamiltonian of the lasing ion without radiation field, and $-\mathbf{d}\cdot\mathbf{E}$ the interaction between the radiation and the medium, in the dipole approximation. Considering one particular radiation whose upper and lower levels are labeled by their angular momentum J and J', respectively, using $\mathbf{d}=\Sigma_q d_q\mathbf{e}_\mathbf{q}$, where $d_{\pm1}=\mp(d_x\pm id_y)/\sqrt{2}$ and $d_0=d_z$, ignoring the energy nonconserving parts generated by the term $\mathbf{d}\cdot\mathbf{E}$ in Eq. (7) [13], and assuming that the coherence envelopes are in quasi-steady-state with respect to their production and decay processes lead to

$$\mathbf{P}_{\sigma+}=-\frac{iEe^{i(\omega t-ky-\pi/2)}}{2\sqrt{2}\hbar}\,\pi\Psi(\omega)\sum_M\,\langle JM|d_1|J'M-1\rangle^2$$
$$\times(n_{JM}-n_{J'M-1})\mathbf{e}_1+\mathrm{H.c.},$$
$$\mathbf{P}_{\sigma-}=\frac{iEe^{-i(\omega t-ky+\pi/2)}}{2\sqrt{2}\hbar}\,\pi\Psi^*(\omega)\sum_M\,\langle JM|d_{-1}|J'M+1\rangle^2$$
$$\times(n_{JM}-n_{J'M+1})\mathbf{e}_1+\mathrm{H.c.},$$
$$\mathbf{P}_{\pi}=\frac{Ee^{i(\omega t-ky+\varphi)}}{2\hbar}\,\pi\Psi(\omega)\sum_M\,\langle JM|d_0|J'M\rangle^2$$
$$\times(n_{JM}-n_{J'M})\mathbf{e}_0+\mathrm{H.c.}, \quad (8)$$

where $\pi\Psi(\omega)=[\Phi(\omega)-i\chi(\omega)]/2$ is the complex profile, with $\Phi(\omega)$ designating the usual line profile and $\chi(\omega)$ the dispersion profile.

At this point we make the following remarks, which will simplify the notations in subsequent formulas.

(i) Since $\langle JM|d_q|J'M-q\rangle^2=\langle J'M-q|d_{-q}|JM\rangle^2$ we can choose to always write the matrix elements in the same order, namely the upper JM states in the bra part and the lower $J'M'$ states in the ket part, as in Eqs. (8). For a particular couple of states $JM,J'M'$, this assigns the value of the q index. As a consequence, a unique correspondence appears between the polarization indexes and the q values:

$$\sigma+\Leftrightarrow q=1,$$
$$\sigma-\Leftrightarrow q=-1,$$
$$\pi\Leftrightarrow q=0,$$

and we shall hereafter designate quantities like intensities $I_{\sigma\pm}$ by $I^{(\pm1)}$, I_π by $I^{(0)}$ (with an upper index to avoid any confusion with a vectorial component), and so on.

(ii) The field polarized along x being $\mathbf{E}_{\sigma+}+\mathbf{E}_{\sigma-}$ [Eqs. (4a) and 4(b)], the corresponding intensity I_x is

$$\varepsilon_0 c\,\frac{1}{T}\int_0^T dt(\mathbf{E}_{\sigma+}+\mathbf{E}_{\sigma-})\cdot(\mathbf{E}_{\sigma+}+\mathbf{E}_{\sigma-}).$$

Now $\mathbf{E}_{\sigma+}\cdot\mathbf{E}_{\sigma-}=-(E^2/4)\cos[2(\omega t-ky)]$ gives no contribution to the integral, and $I_x=I^{(1)}+I^{(-1)}$. With this convention the total intensity is then

$$I=\sum_q\,I^{(q)}.$$

Reporting Eqs. (8) in Eq. (3), applying the paraxial approximation, and using the time-retarded variable $t-y/c$ [13,14] leads to the radiative-transfer equation accounting for induced and spontaneous emissions, and absorption:

$$\frac{\partial}{\partial y} I^{(q)}_{J,J'}(\nu,y,t) = j^{(q)}_{J,J'}(\nu,y,t) + G^{(q)}_{J,J'}(\nu,y,t) I^{(q)}_{J,J'}(\nu,y,t), \tag{9}$$

where $j^{(q)}_{J,J'}$ and $G^{(q)}_{J,J'}$, are, respectively, the monochromatic emissivity and gain corresponding to a given polarization, both of which depend on y for large intensities. In our study the emissivity corresponds to the fraction of radiation spontaneously generated in a small solid angle θ (≈ 10 mrad) centered on the y axis. It involves all the transitions $JM - J'M'$ such that $M - M' = q$, and may be written

$$j^{(q)}_{J,J'}(\nu,y,t) = \frac{3\theta}{8\pi}(2J+1) A_{J,J'} h\nu \Phi_{J,J'}(\nu) \sum_M n_{JM}(y,t) \times \begin{pmatrix} J & 1 & J' \\ -M & q & M-q \end{pmatrix}^2, \tag{10}$$

where $A_{J,J'}$ is the rate of spontaneous emission from the J to the J' level. The local gain is written as [14]

$$G^{(q)}_{J,J'}(\nu,y,t) = \frac{k}{2\varepsilon_0 \hbar} \Phi_{J,J'}(\nu) \sum_M \langle JM|d_q|J'M-q\rangle^2 \times [n_{JM}(y,t) - n_{J'M-q}(y,t)]. \tag{11}$$

Equation (7) gives the rate equations that describe the evolution of the fractional-population densities n in the presence of the radiation resulting from the $JM - J'M'$ transitions:

$$\begin{aligned} \frac{\partial}{\partial t} n_{JM}(y,t) = {} & r_{JM}(t) - \Gamma_{JM}(t) n_{JM}(y,t) \\ & - \sum_q \langle JM|d_q|J'M-q\rangle^2 \\ & \times [n_{JM}(y,t) - n_{J'M-q}(y,t)] \\ & \times \frac{1}{2\hbar^2 \varepsilon_0 c} \int d\nu I^{(q)}_{J,J'}(\nu,y,t) \Phi_{J,J'}(\nu) \end{aligned} \tag{12}$$

for the upper states and

$$\begin{aligned} \frac{\partial}{\partial t} n_{J'M'}(y,t) = {} & r_{J'M'}(t) - \Gamma_{J'M'}(t) n_{J'M'}(y,t) \\ & + \sum_q \langle JM'+q|d_q|J'M'\rangle^2 \\ & \times [n_{JM'+q}(y,t) - n_{J'M'}(y,t)] \\ & \times \frac{1}{2\hbar^2 \varepsilon_0 c} \int d\nu I^{(q)}_{J,J'}(\nu,y,t) \Phi_{J,J'}(\nu) \end{aligned} \tag{13}$$

for the lower states. These equations determine the populations of the quantum states and generalize the usual system of equations that governs the evolution of the energy-level populations. The r and Γ coefficients arise from all populating and depopulating processes, except those of absorption and stimulated emission. The last contribution in both equations represents the effect of the x-ray beam on the quantum-state populations. $I^{(q)}_{J,J'}$ is the intensity contribution due to waves in a given (fixed q) polarization state. It involves the transitions $|JM\rangle \rightarrow |J'M-q\rangle$. The normalized profile $\Phi_{J,J'}$ is calculated numerically according to Ref. [15]. It has been checked that the Stark broadening due to neighboring ions as well as the electron-impact broadening are very small for the investigated cases ($3p$-$3s$ transitions in Ne-like Ge).

Using the property $\langle JM|d_1|J'M-1\rangle^2 = \langle J-M|d_{-1}|J'-M+1\rangle^2$, and dropping the y and t coordinates, we can obtain the rate equations in the presence of the 0-1 and 2-1 radiations:

$$\begin{aligned} \frac{\partial}{\partial t} n_{2\pm2} &= r_{2\pm2} - \Gamma_{2\pm2} n_{2\pm2} - [n_{2\pm2} - n_{1\pm1}] 3\Lambda^{(\pm1)}_{2,1}, \\ \frac{\partial}{\partial t} n_{2\pm1} &= r_{2\pm1} - \Gamma_{2\pm1} n_{2\pm1} - [n_{2\pm1} - n_{10}] \tfrac{3}{2} \Lambda^{(\pm1)}_{2,1} - [n_{2\pm1} - n_{1\pm1}] \tfrac{3}{2} \Lambda^{(0)}_{2,1}, \\ \frac{\partial}{\partial t} n_{20} &= r_{20} - \Gamma_{20} n_{20} - [n_{20} - n_{11}] \tfrac{1}{2} \Lambda^{(-1)}_{2,1} - [n_{20} - n_{1-1}] \tfrac{1}{2} \Lambda^{(1)}_{2,1} - [n_{20} - n_{10}] 2\Lambda^{(0)}_{2,1}, \\ \frac{\partial}{\partial t} n_{1\pm1} &= r_{1\pm1} - \Gamma_{1\pm1} n_{1\pm1} + [n_{2\pm2} - n_{1\pm1}] 3\Lambda^{(\pm1)}_{2,1} + [n_{20} - n_{1\pm1}] \tfrac{1}{2} \Lambda^{(\mp1)}_{2,1} + [n_{2\pm1} - n_{1\pm1}] \tfrac{3}{2} \Lambda^{(0)}_{2,1} + [n_{00} - n_{1\pm1}] \Lambda^{(\mp1)}_{0,1}, \\ \frac{\partial}{\partial t} n_{10} &= r_{10} - \Gamma_{10} n_{10} + [n_{21} - n_{10}] \tfrac{3}{2} \Lambda^{(1)}_{2,1} + [n_{2-1} - n_{10}] \times \tfrac{3}{2} \Lambda^{(-1)}_{2,1} + [n_{20} - n_{10}] 2\Lambda^{(0)}_{2,1} + [n_{00} - n_{10}] \Lambda^{(0)}_{0,1}, \\ \frac{\partial}{\partial t} n_{00} &= r_{00} - \Gamma_{00} n_{00} - [n_{00} - n_{11}] \Lambda^{(-1)}_{0,1} - [n_{00} - n_{1-1}] \Lambda^{(1)}_{0,1} - [n_{00} - n_{10}] \Lambda^{(0)}_{0,1}, \end{aligned} \tag{14}$$

with

$$\Lambda^{(q)}_{J,J'}[= \Lambda^{(q)}_{J,J'}(y,t)] = \frac{B_{J,J'}}{c} \int d\nu I^{(q)}_{J,J'}(\nu,y,t) \Phi_{J,J'}(\nu), \tag{15}$$

where $B_{J,J'} = (J\|d\|J')^2/[6\hbar^2\varepsilon_0(2J+1)]$ is the Einstein coefficient for stimulated emission. The spontaneous emission is known to be isotropic, and we reasonably assume that the electron-ion collisions also verify this property, yielding $r_{JM} = r_{J-M}$ and $\Gamma_{JM} = \Gamma_{J-M}$. Moreover, without incident radiation or with a totally unpolarized radiation, the $\Lambda^{(q)}_{J,J'}$ integrals do not depend on q. The systems of rate equations for the $\{|JM\rangle, |J'M'\rangle\}_{M,M' \geq 0}$ and $\{|JM\rangle, |J', M'\rangle\}_{M,M' \leq 0}$ groups of states are then identical, giving $n_{JM} = n_{J-M}$ and $n_{J'M'} = n_{J'-M'}$. The resolution of the rate equations then need consider only one sign, e.g., the upper sign.

The radiative-transfer problem is solved by partitioning the plasma column into a succession of m adjacent cylinders with a common axis y and lengths $y_p - y_{p-1}$ ($p = 1,2,...,m$). $y_m - y_0$ is the total plasma length. The intervals

are chosen sufficiently small so that the populations, temperatures, and densities are independent of y in each cylinder. In a given interval $[y_{p-1},y_p]$ the equation of transfer is then easily integrated, yielding

$$I^{(q)}(y)=\frac{j^{(q)}(y_p)}{G^{(q)}(y_p)}\{\exp[G^{(q)}(y_p)(y-y_{p-1})]-1\}+I^{(q)}(y_{p-1})\exp[G^{(q)}(y_p)(y-y_{p-1})], \quad (16)$$

where the time and frequency variables are omitted. The first contribution on the right-hand side rhs of the above equation is due to the emission spontaneously generated and amplified in the considered interval, while the second describes the amplification, in the same interval, of the radiation coming from the preceding segment $[y_{p-2},y_{p-1}]$. Assuming $I^{(q)}(y_0)=0$ (no incident radiation), we easily obtain the output intensity in terms of the source function $S^{(q)}(y)=[j^{(q)}(y)]/[G^{(q)}(y)]$ and spectral gain, at the various abscissae y_p:

$$I^{(q)}(y_m)=\sum_{p=1}^{m}[S^{(q)}(y_p)-S^{(q)}(y_{p-1})]\times\exp\sum_{l=p}^{m}[G^{(q)}(y_l)(y_l-y_{l-1})]-S^{(q)}(y_m), \quad (17)$$

with the condition $S^{(q)}(y_0)=0$.

In order to account for the Λ integrals that describe the effect of the lasing radiation on the quantum-state populations, the set of population equations [Eq. (14)] is resolved by a postprocessor coupled to the 1.5-D hydrodynamics–atomic physics code EHYBRID [16]. The hydrodynamic quantities of interest are provided by the EHYBRID code, which considers the single-sided illumination of a slab target. The plasma is typically divided into 98 Lagrangian cells in the direction parallel to the pump laser; its expansion in the transverse dimension is assumed to be self-similar, each cell being considered isothermal. The incoming laser energy is absorbed by inverse bremsstrahlung and resonant absorption at the critical surface. The rates contained in the population equations involve all significant interlevel terms and have yielded a very satisfactory description of the laser in the small-signal limit [17]. The problem is modeled in a piecewise fashion through the plasma column, assuming uniform conditions inside each interval, for the purpose of (i) finding the atomic populations and (ii) amplifying the beam through the section of plasma thus obtained, appending the appropriate ASE term from the segment. We assume that an aperture of 10 mrad of the spontaneous emission contributes to the x-ray beam. The populations are calculated in the steady-state approximation.

III. LINEAR POLARIZATION

The degree of polarization $D(-1\leqslant D\leqslant 1)$ is conventionally defined as

$$D(y)=\frac{I_{\parallel}(y)-I_{\perp}(y)}{I_{\parallel}(y)+I_{\perp}(y)}, \quad (18)$$

where $I_{\parallel}$ and $I_{\perp}$ are the frequency-integrated intensities, with the direction of polarization along the x and the z axes, respectively. As indicated above we simply have $I_{\parallel}=I^{(1)}+I^{(-1)}$ and $I_{\perp}=I^{(0)}$.

Dealing with quantum-state populations rather than with level populations, elastic electron-ion collisions of the type $(2p^5 3s)_{1M}+e^-\rightarrow(2p^5 3s)_{1M'}+e^-$, with $M\neq M'$, must be taken into account. An estimation of the rate of elastic collisions with momentum transfer is given by the useful formula [18]

$$\Omega(\mathrm{s}^{-1})\approx 3.87\times 10^{-6}N_{\mathrm{elec}}(\mathrm{cm}^{-3})Z[T_e(\mathrm{eV})]^{-3/2}\ln\Lambda, \quad (19)$$

where Z is the ion charge, T_e the electron temperature, and $\ln\Lambda$ the Coulomb logarithm. The effect of these collisions is to restore equilibrium between the populations of the various quantum states associated with each level. In other words, they attenuate or even, as seen below, eliminate the population differences that might be induced by the x-ray field.

In view of comparison with the experiment of Rus *et al.* [11], we have resolved the system of equations giving the intensity of the 2-1 radiation, in the presence of the 0-1 radiation. In fact, these transitions share the same lower level and have to be considered in the same calculation. The electron and ion temperatures and the electron density are obtained with the help of EHYBRID. The intensity of the x-ray beams remains below the saturation threshold. The electric field of the linearly polarized beam, which is injected in the amplifier, is written as a coherent superposition of a σ_+ and a σ_- wave, and is directed along the x axis, assuming an appropriate phase difference (see Sec. II). The corresponding intensity is simply the sum of the two equal intensities $I^{(1)}$ and $I^{(-1)}$. In this case we have $\Lambda^{(1)}_{J,J'}=\Lambda^{(-1)}_{J,J'}$, and the symmetry $M\leftrightarrow -M$ is statistically preserved by the physical processes. We have accordingly $n_{JM}=n_{J-M}$ and $n_{J'M'}=n_{J'-M'}$, and the resolution of the rate equations need consider only one sign, e.g., the upper sign:

$$\frac{\partial}{\partial t}n_{22}=r_{22}-\Gamma_{22}n_{22}-[n_{22}-n_{11}]3\Lambda^{(1)}_{2,1},$$

$$\frac{\partial}{\partial t}n_{21}=r_{21}-\Gamma_{21}n_{21}-[n_{21}-n_{10}]\tfrac{3}{2}\Lambda^{(1)}_{2,1}-[n_{21}-n_{11}]\tfrac{3}{2}\Lambda^{(0)}_{2,1},$$

$$\frac{\partial}{\partial t}n_{20}=r_{20}-\Gamma_{20}n_{20}-[n_{20}-n_{11}]\Lambda^{(1)}_{2,1}-[n_{20}-n_{10}]2\Lambda^{(0)}_{2,1},$$

$$\frac{\partial}{\partial t}n_{11}=r_{11}-\Gamma_{11}n_{11}+[n_{22}-n_{11}]3\Lambda^{(1)}_{2,1}+[n_{20}-n_{11}]\tfrac{1}{2}\Lambda^{(1)}_{2,1}+[n_{00}-n_{11}]\Lambda^{(1)}_{0,1}+[n_{21}-n_{11}]\tfrac{3}{2}\Lambda^{(0)}_{2,1},$$

$$\frac{\partial}{\partial t}n_{10}=r_{10}-\Gamma_{10}n_{10}+[n_{21}-n_{10}]3\Lambda^{(1)}_{2,1}+[n_{20}-n_{10}]2\Lambda^{(0)}_{2,1}+[n_{00}-n_{10}]\Lambda^{(0)}_{0,1},$$

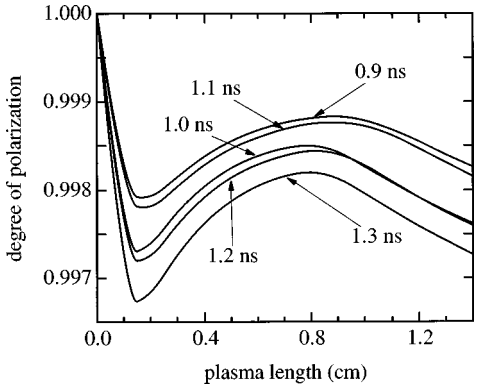

FIG. 3. Degree of polarization of the Ne-like Ge 2-1 radiation (23.6 nm), as a function of plasma length for various times ranging in the laser pulse duration. The irradiation conditions and the dimensions of the two slab targets (injector+amplifier) are identical to those of the experiment of Rus *et al.* [11]. 1.1 ns is the time at which the pump laser delivers its maximal intensity.

$$\frac{\partial}{\partial t} n_{00} = r_{00} - \Gamma_{00} n_{00} - [n_{00} - n_{11}] 2\Lambda_{0,1}^{(1)} - [n_{00} - n_{10}] \Lambda_{0,1}^{(0)}. \tag{20}$$

One can show that when the symmetry $M \leftrightarrow -M$ is preserved, and as long as the intensity remains below the saturation regime, the phase variations of the τ_+ and τ_- waves along the propagation axis are equal. Therefore the phase difference of the τ_+ and τ_- waves does not depend on y, and during amplification the electric field of the injected beam remains parallel to the x axis.

Figure 3 shows, for various times, the degree of polarization of the Ne-like Ge 2-1 radiation. The median time 1.1 ns corresponds to the peak of the pump-laser irradiation. As clearly seen, D remains very close to unity, confirming the experimental observation according to which the injected radiation does not suffer a measurable degradation of its polarization state. D decreases slightly from unity for small values of y due to the apparition of the spontaneously emitted π wave. However, owing to the seeded beam, the increase is more important for the circularly polarized waves, yielding an increase of D for sufficiently large plasma lengths. This behavior is obtained for all values of time. It must be noted that these variations are too small to be observed.

Let us now consider the 0-1 radiation. For the same reason as above, the resolution of the population equations should account for the 2-1 radiation as well. A hydrodynamic simulation using EHYBRID with the same irradiance as in the experiment of Kawachi *et al.* [12], namely 3×10^{13} W cm^{-2}, provides the electron and ion temperatures and the electron density that are used in the paraxial MB calculation. These quantities, as well as the ion density, are transiently close to the estimations of Kawachi *et al.*, namely $T_e = 450$ eV, $T_i = 100$ eV, $N_{\text{elec}} = 6.75 \times 10^{19}$ cm^{-3}, and $N_{\text{ion}} = 3.14 \times 10^{18}$ cm^{-3}. The agreement is also good for the Ne-like ground-state population density $N_g (= 1.18 \times 10^{18}$ cm$^{-3})$, $N_{1M} (= 8 \times 10^{13}$ cm$^{-3})$, and $N_{00} (= 1.38 \times 10^{15}$ cm$^{-3})$, giving rise to a local gain of 2.7 cm^{-1}, a value identical to the gain obtained by Kawachi *et al.* On this basis we can now consider the possible effect on the populations N_{1M}, of the trapping of the resonance line (lower level→ground level: $1 \rightarrow g$), as considered in Ref. [12]. We study quantum-state populations rather than level populations, and it is thus necessary to account for elastic electron-ion collisions. It can be readily seen that for elastic collisions, such that $|1M\rangle + e^- \rightarrow |1M'\rangle + e^-$ with $M \neq M'$, the selection rules are identical to those of the electric quadrupole $-E2$ transitions. It follows that the transitions between pure $(2p_{1/2}^5 3s_{1/2})_{1M}$ states are forbidden. Now, real states are not pure j-j coupling and contain a $(2p_{3/2}^5 3s_{1/2})_{1M}$ component that renders the transition possible. To have an upper-bound estimation of the effect resulting from the preferential trapping of one component of the radiation, we can ignore the trapping of the other component and use an overestimated value of the intensity of the trapped component. In the geometry of Ref. [12] (where z and x are permuted with respect to Fig. 1 of the present paper) the trapped component is the π wave emitted in the direction perpendicular to the direction of the laser producing the plasma. So, assuming that all the π photons of the $1 \rightarrow g$ line emitted in a narrow slice ($0 \leqslant \phi \leqslant 2\pi$ and $\pi/2 - 0.05 \leqslant \theta \leqslant \pi/2 + 0.05$) perpendicular to the z axis are reabsorbed, the resulting feeding of $(2p^5 3s)_{10}$ is equal to $(3/8\pi) n_{10} A_{1g} 0.6275$. We have included this additional term in the collisional-radiative code. The populations of the quantum states involved in the 0-1 radiation, and the local gains corresponding to the x and z directions are presented in Table I. It is clear that the trapping has no effect on these quantities. For a 3-cm-long plasma these results give an intensity ratio (with trapping) extremely close to 1 (1.03), compared to 3.3 detected by Kawachi *et al.*, who attributed the observed polarization to the radiation-trapping effect here considered. It appears that this effect is in fact quite negligible in the present case, and the intensity ratio of 3.3 must result from other processes.

TABLE I. Population density (in cm^{-3}) of the upper $[(2p^5 3p)_{00}]$ and lower $[(2p^5 3s)_{1M}]$ states involved in the Ne-like Ge 0-1 radiation (19.6 nm), and gains (in cm^{-1}) corresponding to two orthogonal directions. $G_\perp$ and $G_\parallel$ refer to the notation of Kawachi *et al.* [12].

	Without trapping	With trapping
N_{00}	1.38×10^{15}	1.38×10^{15}
$N_{1\pm1}$	8.16×10^{13}	8.17×10^{13}
N_{10}	8.16×10^{13}	8.72×10^{13}
$G_\perp$	2.70	2.70
$G_\parallel$	2.70	2.69

IV. CIRCULAR POLARIZATION

In the above section we have shown that the polarization state of the output is identical to that of the incident beam if the latter is linearly polarized. This result is confirmed by experiment. It is also important to study the influence of a circularly polarized incident beam, and of elastic electron-ion collisions, on the output polarization. A related objective, showing the effect of the injected beam on the ability of the plasma to generate a spontaneous polarization, is considered through the behavior of the atomic orientation and alignment. We choose the system of axes as follows: the z axis is

taken to be the propagation axis, and then only circularly polarized waves can propagate.

The MB equations, including the radiative-transfer equation, allow us to investigate the fractional populations—diagonal elements of the density matrix—of the various states associated with each level. In numerous situations it is more advantageous to consider the tensorial components $\rho_Q^{(K)}(J)$ of the density matrix, defined by [19]

$$\rho_Q^{(K)}(J)=\sum_{M,M'}(-1)^{J-M}\sqrt{2K+1}\times\begin{pmatrix} J & K & J \\ -M & Q & M' \end{pmatrix}\rho_{JM,JM'}. \tag{21}$$

K is a positive or null integer ranging from 0 to $2J$, and Q a relative integer ranging from $-K$ to K. From Eq. (21) we readily obtain

$$\rho_{JM,JM'}=\sum_{K,Q}(-1)^{J-M}\sqrt{2K+1}\begin{pmatrix} J & K & J \\ -M & Q & M' \end{pmatrix}\rho_Q^{(K)}(J). \tag{22}$$

The $\rho_0^{(0)}(J)$ component is called population because it is simply proportional to the overall population of the J level. The $\rho_0^{(1)}(J)$ component is called orientation because it is proportional to the weighted average value of the z component of the angular momentum **J**. Finally, the $\rho_0^{(2)}(J)$ component is called alignment. It describes the anisotropy of the medium. It is obvious that for $J=0$ orientation and alignment are always zero. We have for $J\neq 0$

$$\rho_0^{(0)}(J)=\frac{1}{\sqrt{2J+1}}\sum_M n_{JM}, \tag{23a}$$

$$\rho_0^{(1)}(J)=2\sqrt{3\frac{(2J-1)!}{(2J+2)!}}\sum_M Mn_{JM}, \tag{23b}$$

$$\rho_0^{(2)}(J)=2\sqrt{5\frac{(2J-2)!}{(2J+3)!}}\sum_M [3M^2-J(J+1)]n_{JM}. \tag{23c}$$

When the n_{JM} populations do not depend on M, orientation and alignment are equal to zero because $\Sigma_M M=\Sigma_M[3M^2-J(J+1)]=0$. The emerging beam is thus unpolarized if its intensity is integrated over a sufficiently large time interval. If now n_{JM} depends on M but the condition $n_{JM}=n_{J-M}$ is still fulfilled, the orientation is zero and the alignment is finite. In this case the output may only be linearly polarized or unpolarized. When the elastic electron-ion collisions have a negligible effect on the populations (small density), the radiation that propagates along the z axis and that is associated with a nonzero orientation is circularly polarized, while with a zero orientation (implying $I^{(1)}=I^{(-1)}$) and a nonzero alignment it is either unpolarized or linearly polarized. It is worth noting that without any external radiation penetrating into the plasma, we have $\Lambda_{J,J'}^{(q)}=\Lambda_{J,J'}^{(-q)}$, and the populations are symmetrical with respect to the transformation $M\leftrightarrow -M$ [see Eq. (20)]. We then have $\rho_0^{(1)}=0$, and the output could only be linearly polarized or unpolarized.

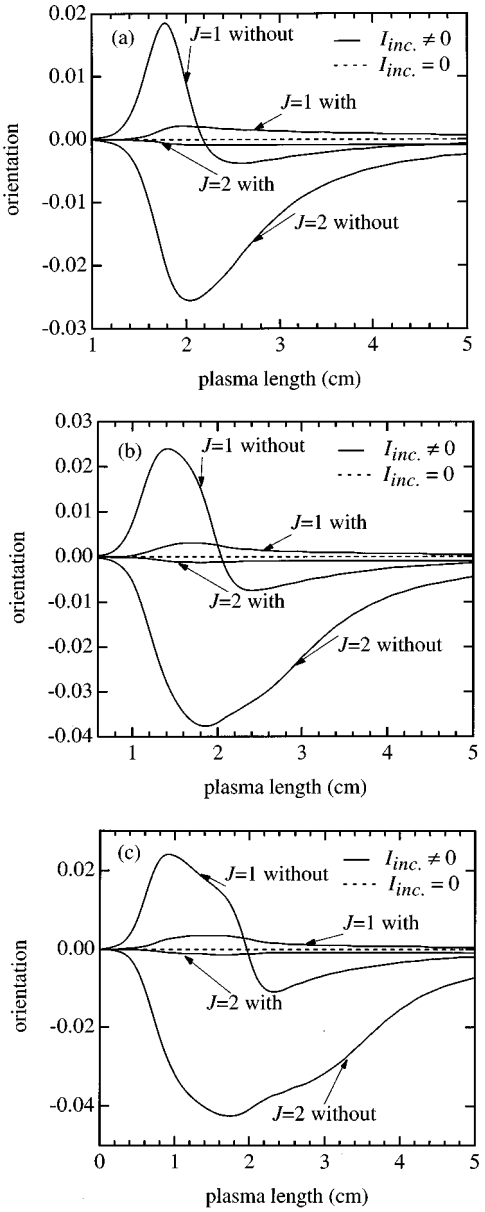

FIG. 4. Orientation of the Ne-like Ge ions, as a function of plasma length, when an incident τ_+ 2-1 beam with intensity $I_{\text{inc.}}$ (output of the injector) is coupled to the amplifier. The injector lengths are (a) 0.5 cm, (b) 1 cm, and (c) 1.5 cm. ''With'' and ''without'' mean with and without elastic electron-ion collisions. The dashed curve shows the orientation in the absence of incident beam ($I_{\text{inc.}}=0$). Electron density equals 7×10^{20} cm^{-3}, electron and ion temperatures are, respectively, 500 and 300 eV.

When a circularly polarized radiation is injected in an amplifying plasma the populations are no longer symmetrical and the orientation is finite.

Figure 4 shows the development of the orientation of the $J=1$ and $J=2$ levels in plasma conditions where saturation occurs: $N_{\text{elec}}=7\times10^{20}$ cm^{-3}, $T_e=500$ eV, and $T_i=300$ eV. These conditions may be obtained with the use of curved targets or prepulses. A Ne-like Ge 2-1 radiation (23.6 nm), right-circularly polarized, is seeded in an amplifying plasma after propagation in an injector of length (a) 0.5 cm, (b) 1 cm, and (c) 1.5 cm. The comparison of the curves obtained with elastic collisions $|JM\rangle+e^-\rightarrow|JM'\rangle+e^-(M'\neq M)$

taken into account (''with'') or ignored (''without'') exhibits the effects of these collisions on population distribution and therefore on orientation. When the elastic collisions are ignored we see that the injected beam begins to affect differently the quantum-state populations when attaining its saturation threshold. This occurs at a length of 1 cm in the amplifying plasma in case (a), 0.6 cm in case (b), while for a preamplification in a 1.5-cm-long injector (c) the length nears 0.1 cm. The curves have the same shape.

The orientation of the $J=2$ level is negative due to the incident τ_+ radiation, which makes the intensity $I^{(1)}$ much larger than $I^{(-1)}$, yielding a more important depopulation for the $M \geqslant 0$ states than for the $M<0$ ones. The orientation of this level begins to decrease for increasing plasma length as $I^{(1)}$ is saturating, the depletion of states being stronger for higher M values [see the relative line strengths in Fig. 2(b)], while $I^{(-1)}$ remains below saturation. At higher z values saturation is achieved for $I^{(1)}$, and $I^{(-1)}$ itself begins to gradually saturate, yielding a smaller and smaller $|n_{2M}-n_{2-M}|$ difference. Consequently, we observe a reduction of the orientation that asymptotically tends to zero.

A quite opposite effect is noticed for the lower level. Under the dominant τ_+ radiation, to the most depleted upper states $|2M\rangle$ correspond the most fed lower states $|1M-1\rangle$. As a result, $|11\rangle$ is more fed than $|1-1\rangle$, and the orientation is positive. The minimal plasma length at which the orientation becomes finite decreases for increasing seeded intensities. As above, when complete saturation is achieved the populations of the various $|1M\rangle$ states are no longer different, and the orientation tends to a finite limit.

Figure 5 shows the alignment for the same plasma parameters as above. Considering the $J=1$ level, the alignment is proportional to $n_{11}+n_{1-1}-2n_{10}$. When the elastic collisions are ignored we notice in case (a) [Fig. 5(a)] a rapid increase near 1.4 cm. This is mainly due to the 0-1 radiation, which saturates first and rapidly increases $n_{1\pm1}$, yielding a positive alignment. In cases (b) and (c), it is the injected $\sigma+$ 2-1 radiation that saturates first. The differences between the evolutions of n_{11}, n_{10}, and n_{1-1} is then the main cause of the transiently negative alignment. From Eqs. (14) the population rate due to the $\sigma+$ 2-1 radiation is $3[n_{22}-n_{11}]\Lambda^{(1)}_{2,1}$ for n_{11}, $\frac{3}{2}[n_{21}-n_{10}]\Lambda^{(1)}_{2,1}$, for n_{10}, and $\frac{1}{2}[n_{20}-n_{1-1}]\Lambda^{(1)}_{2,1}$ for n_{1-1}. Now, as indicated above, $n_{22}<n_{21}<n_{20}$ and $n_{11}>n_{10}>n_{1-1}$, so that $3[n_{22}-n_{11}]+\frac{1}{2}[n_{20}-n_{1-1}]-2\frac{3}{2}[n_{21}-n_{10}]$ is transiently negative. At greater length, the alignment becomes positive under the influence of 0-1, as in case (a). The important effect of 0-1 is clearly exhibited in the absence of external radiation. At even greater length the influence of the spontaneously generated $\sigma-$ 2-1 reequilibrates the populations, therefore lessening the alignment. Due to saturation above a certain plasma length, the populations no longer vary and the alignment tends to a limit.

Similar considerations explain the behavior of the $J=2$-level alignment, which is proportional to $6(n_{22}+n_{2-2})-3(n_{21}+n_{2-1})-6n_{20}$. The populations not being directly concerned by 0-1, the alignment remains everywhere less pronounced than for the $J=1$ level. In all cases, orientation and alignment are strongly attenuated by elastic electron-ion collisions.

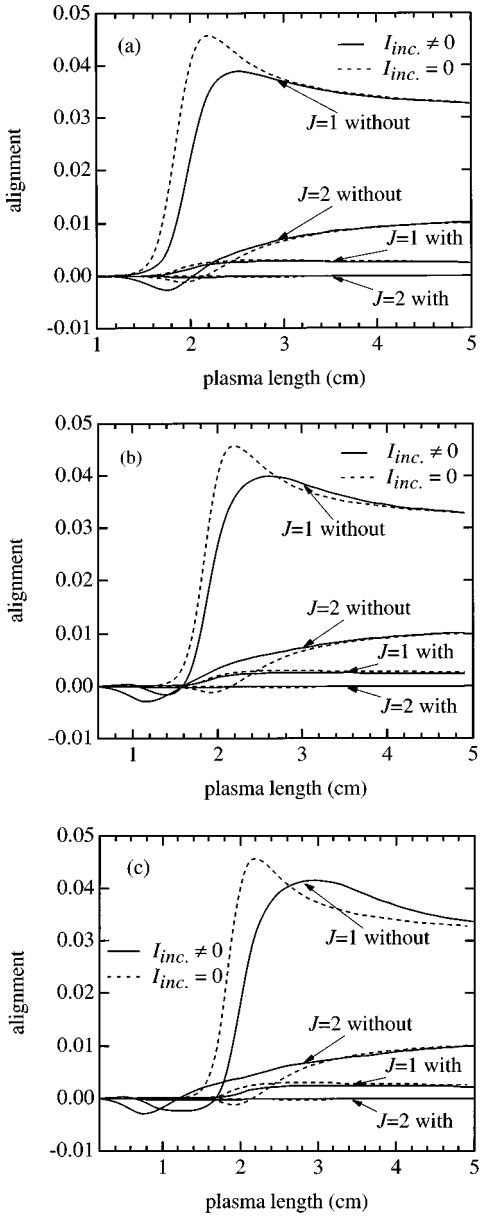

FIG. 5. Alignment of the Ne-like Ge ions, as a function of plasma length, same as in Fig. 4.

We now focus our attention on the output polarization. The two waves τ_+ and τ_- are independent of each other (no phase relation), and their coherency matrices [20] are, respectively,

$$C^{(1)}=\frac{I^{(1)}}{2}\begin{pmatrix}1 & i\\ -i & 1\end{pmatrix}, \quad C^{(-1)}=\frac{I^{(-1)}}{2}\begin{pmatrix}1 & -i\\ i & 1\end{pmatrix}. \quad (24)$$

As the waves are independent of each other, the coherency matrix C of the output is simply the sum of the above matrices:

$$C=\frac{1}{2}\begin{pmatrix}I^{(1)}+I^{(-1)} & i[I^{(1)}-I^{(-1)}]\\ -i[I^{(1)}-I^{(-1)}] & I^{(1)}+I^{(-1)}\end{pmatrix}. \quad (25)$$

Any quasimonochromatic radiation may be expressed as the sum of a completely unpolarized and a completely polarized wave, which are independent of each other, and the decom-

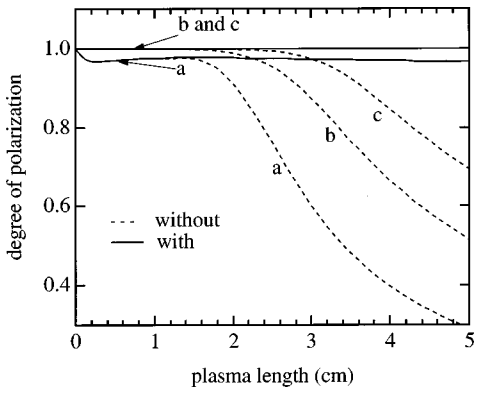

FIG. 6. Degree of polarization of the Ne-like Ge 2-1 radiation (23.6 nm), as a function of plasma length, when an incident τ_+ 2-1 beam (output of the injector) is coupled to the amplifier. The injector lengths are (a) 0.5 cm, (b) 1 cm, and (c) 1.5 cm. Full curves account for elastic electron-ion collisions and dashed curves ignore them. Temperatures and density as in Fig. 4.

position is unique. The coherency matrix of the unpolarized component is of the form $A\mathbf{1}$, where A is positive real and $\mathbf{1}$ the 2×2 identity matrix, that of the polarized component has its diagonal formed of positive reals, while the other two matrix elements are complex conjugates of each other. The degree of polarization of the emerging radiation, defined as the ratio of the intensity of the polarized portion to the total intensity, is given by [20]

$$D=\sqrt{1-4\frac{\mathrm{Det}\ C}{(C_{11}+C_{22})^2}}. \tag{26}$$

It is then easy to show that $D=|I^{(1)}-I^{(-1)}|/[I^{(1)}+I^{(-1)}]$.

Figure 6 shows the degree of polarization of the Ne-like Ge 2-1 radiation. In the absence of elastic electron-ion collisions the degree of polarization of the output is smaller than that of the injected τ_+ beam, i.e., 1. In fact, due to a finite orientation (see Fig. 4), the medium is able to generate a σ_- wave with a significant intensity. It is clear that the contribution of this wave to the D value diminishes when the intensity of the seeded wave is increased. As a result, D tends to the limit value 1. When elastic collisions are taken into account, the degree of polarization remains close to the D value of the incident beam. In other words, when elastic collisions are taken into account the medium has a negligible effect on the output polarization (negligible orientation).

V. CONCLUSION

This work investigates the influence of an amplifying plasma on the polarization state of X-UV radiation. When the amplified-beam intensity approaches saturation it modifies the polarization properties of the medium, and this effect is studied in terms of orientation and alignment. The coupled intensity and population equations are resolved with the help of the MB theory, which is the most convenient tool for plasma samples exhibiting population inversions between two groups of quantum states connected by electric-dipole interaction. The equations are valid even if a radiation in a definite polarization state is injected in the amplifier, provided the coherence envelopes are assumed to be in steady state with respect to their production and decay processes. When the ASE intensities become large, this approach is appropriate to describe the continuous transition to saturation of x-ray lasers in plasmas.

Our calculations have been applied to germanium slab targets, which, in the $3p$-$3s$ scheme of the Ne-like sequence, allow one of the highest efficiencies in collisionally pumped lasers with large gain-length products. We have shown that a linearly polarized beam, coupled to an amplifying plasma, does not suffer a measurable degradation of its polarization state. Our results for the 2-1 line are in good agreement with the measurement of Rus *et al.* [11]. Concerning the 0-1 line, the experiment of Kawachi *et al.* [12] has shown an important degree of polarization, which was explained by the authors as resulting from a selective photon trapping of the resonance line, due to a preferential direction of expansion. The populations of the lower laser states, calculated with radiation trapping taken into account, do not show sufficiently large relative differences to explain the observed polarization. Moreover, the small effect of photon trapping is strongly attenuated by the elastic electron-ion collisions, which tend to equalize the quantum-state populations associated with each level.

We have also calculated the orientation and alignment of a lasing plasma in a configuration of injector-amplifier. With an incident τ_+ beam the orientation is finite in the absence of elastic electron-ion collisions, and the medium gives rise to τ_+ and τ_- waves. As a result, the degree of polarization of the output is less than that of the incident beam, i.e., 1. If elastic collisions are taken into account, the orientation is negligible and the medium has no effect on the polarization. In this case the degree of polarization of the emerging signal is equal to that of the incident wave.

In order to estimate the influence of the medium on the output polarization and to evaluate the role of elastic collisions, we plan an experiment at the Laboratoire pour l'Utilisation des Lasers Intenses laser facility (École Polytechnique) in an injector-amplifier configuration. Multilayer mirrors will be used to polarize the injector—unpolarized—output, providing a circularly polarized beam at the entry of the amplifier.

ACKNOWLEDGMENTS

We are very grateful to G. J. Pert (York University) for providing the EHYBRID code that has been used in the hydrodynamic calculation. We are also pleased to acknowledge useful discussions during this work with G. Jamelot and Ph. Zeitoun (LSAI, Université Paris–Sud).

[1] D. L. Matthews, P. L. Hagelstein, M. D. Rosen, M. J. Eckart, N. M. Ceglio, A. Hazi, H. Medecki, B. J. McGowan, J. E. Trebes, B. L. Whitten, E. M. Campbell, C. W. Hatcher, A. M. Hawryluk, R. L. Kauffman, L. D. Plaseance, G. Rambach, G. H. Scofield, G. Stone, and T. Weaver, Phys. Rev. Lett. **54**, 110 (1985).

[2] E. E. Fill, Y. Li, P. X. Lu, and G. Pretzler, in *X-ray Lasers 1996, Proceedings of the Fifth International Colloquium on*

X-ray Lasers, edited by S. Svanberg and C.-G. Wahlström, IOP Conf. Ser. No. 151 (Institute of Physics, Bristol, 1996), p. 25.

[3] B. J. MacGowan, L. B. DaSilva, D. J. Fields, C. J. Keane, J. A. Koch, R. A. London, D. L. Matthews, S. Maxon, S. Mrowka, A. L. Osterheld, J. H. Scofield, G. Shimkaveg, J. E. Trebes, and R. S. Walling, Phys. Fluids B **4**, 2326 (1992).

[4] J. J. Rocca, D. P. Clark, F. G. Tomasel, V. N. Shlyaptsev, J. L. A. Chilla, B. Benware, C. Moreno, D. Burd, and J. J. Gonzalez, in *X-ray Lasers 1996, Proceedings of the Fifth International Colloquium on X-ray Lasers* (Ref. [2]).

[5] P. Jaeglé, A. Carillon, P. Dhez, P. Goedtkindt, G. Jamelot, A. Klisnick, B. Rus, Ph. Zeitoun, S. Jacquemot, D. Mazataud, A. Mens, and J. P. Chauvineau, in *X-ray Lasers 1994, Proceedings of the Fourth International Colloquium on X-ray Lasers*, edited by D. C. Eder and D. L. Matthews, AIP Conf. Proc. No. 332 (AIP, NY, 1994), p. 25.

[6] A. Carillon, H. Z. Chen, P. Dhez, L. Dwivedi, J. Jacoby, P. Jaeglé, G. Jamelot, J. Zhang, M. H. Key, A. Kidd, A. Klisnick, R. Kodama, J. Krishnan, C. L. S. Lewis, D. Neely, P. Norreys, D. O'Neill, G. J. Pert, S. A. Ramsden, J. P. Raucourt, G. J. Tallents, and J. Uhomoibhi, Phys. Rev. Lett. **68**, 2917 (1992).

[7] G. M. Shimkaveg, M. R. Carter, R. S. Walling, J. M. Ticehurst, R. A. London, and R. E. Stewart, in *X-ray Lasers 1992, Proceedings of the Third International Colloquium on X-ray Lasers*, edited by E. E. Fill, IOP. Conf. Ser. No. 125 (Institute of Physics, Bristol, 1992), p. 61.

[8] J. Zhang, P. J. Warwick, E. Wolfrum, M. H. Key, C. Danson, A. Demir, S. Healy, D. H. Kalantar, N. S. Kim, C. L. S. Lewis, J. Lin, A. G. MacPhee, D. Neely, J. Nilsen, G. J. Pert, R. Smith, G. J. Tallents, and J. S. Wark, Phys. Rev. A **54**, R4653 (1996).

[9] J. Zhang, A. G. MacPhee, J. Nilsen, J. Lin, T. W. Barbee, Jr., C. Danson, M. H. Key, C. L. S. Lewis, D. Neely, R. M. N. O'Rourke, G. J. Pert, R. Smith, G. J. Tallents, J. S. Wark, and E. Wolfrum, Phys. Rev. Lett. **78**, 3856 (1997).

[10] J. C. Kieffer, J. P. Matte, M. Chaker, Y. Beaudoin, C. Y. Chien, S. Coe, G. Mourou, J. Dubau, and M. K. Inal, Phys. Rev. E **48**, 4648 (1993).

[11] B. Rus, C. L. S. Lewis, G. F. Cairns, P. Dhez, P. Jaeglé, M. H. Key, D. Neely, A. G. MacPhee, S. A. Ramsden, C. G. Smith, and A. Sureau, Phys. Rev. A **51**, 2316 (1995).

[12] T. Kawachi, K. Murai, G. Yuan, S. Ninomiya, R. Kodama, H. Daido, Y. Kato, and T. Fujimoto, Phys. Rev. Lett. **75**, 3826 (1995).

[13] A. Sureau and P. B. Holden, Phys. Rev. A **52**, 3110 (1995).

[14] D. Benredjem, A. Sureau, and C. Möller, Phys. Rev. A **55**, 4576 (1997).

[15] B. Talin, A. Calisti, L. Godbert, R. Stamm, L. Klein, and D. Lee, Phys. Rev. A **51**, 1918 (1995).

[16] G. J. Pert, J. Comput. Phys. **39**, 251 (1980).

[17] P. B. Holden, S. B. Healy, M. T. M. Lightbody, G. J. Pert, J. A. Plowes, A. E. Kingston, E. Robertson, C. L. S. Lewis, and D. Neely, J. Phys. B **27**, 341 (1994).

[18] J. L. Delcroix and A. Bers, *Physique des Plasmas* (InterÉditions/CNRS Éditions, Paris, 1994).

[19] E. Landi Degl'Innocenti, V. Bommier, and S. Sahal-Bréchot, Astron. Astrophys. **244**, 391 (1991).

[20] M. Born and E. Wolf, *Principles of Optics* (Pergamon Press, Oxford, 1993).